

Computational Modeling of Snow Avalanche Dynamics: A case study of Teling Nala near Atal Tunnel

Vishal Sharma¹ and Gaurav Bhutani^{1*}

¹School of Mechanical and Materials Engineering, Indian Institute of Technology Mandi, Himachal Pradesh 175075, India
d22051@students.iitmandi.ac.in; gaurav@iitmandi.ac.in

ABSTRACT

A computational study of snow avalanche dynamics is presented in this work for the Teling Nala gully near Atal Tunnel in Indian Himalayas, which is prone to avalanche incidents in winter and spring. The depth-averaged model with the Mohr-Coulomb plastic rheology was solved using the finite-volume method. The open-source TITAN2D code with adaptive mesh refinement was used for tractable numerical simulations for the large region. The impact of internal friction angle, bed friction angle, and the initial volume of the avalanche pile on the dynamics of avalanche flow is studied. The results indicate that while the internal friction angle has minimal influence on avalanche behaviour, the bed friction angle has a significant effect on both avalanche velocity and runout distance. The initial volume of the avalanche pile has a minor effect on the dynamics. The study also presents a worst-case scenario where an avalanche initiates simultaneously from two starting zones. This research contributes to the present understanding of avalanche behaviour at the Teling Nala site which can be utilised for designing avalanche defense structures and conducting a hazard analysis of the region. It is concluded that computational approach using depth-averaged modelling and adaptive mesh refinement provides a tractable method for analysing avalanche dynamics at key sites such as the one chosen in this work.

Keywords: Snow avalanche, Avalanche dynamics, Computational fluid dynamics, Depth-averaged model, Atal tunnel

I. INTRODUCTION

Snow avalanches are one of the most dangerous gravitational hazards in mountain regions causing loss of life and infrastructure worldwide. The prediction of snow avalanche parameters has been previously carried out using statistical methods, however, due to the complexity of avalanche flows and the lack of historical data for all sites, probabilistic models cannot predict flow in all situations. Therefore, to predict the flow variables such as velocity, avalanche debris height, avalanche track, and runout distance, computational modeling of snow avalanche dynamics provides a promising alternative. Depth-averaged (DA) model is one such method, which leads to considerably quick and reliable simulation analysis.

Predicting avalanche dynamics helps in designing appropriate protective structures, provide timely warnings, and helps inform necessary evacuation measures. Snow

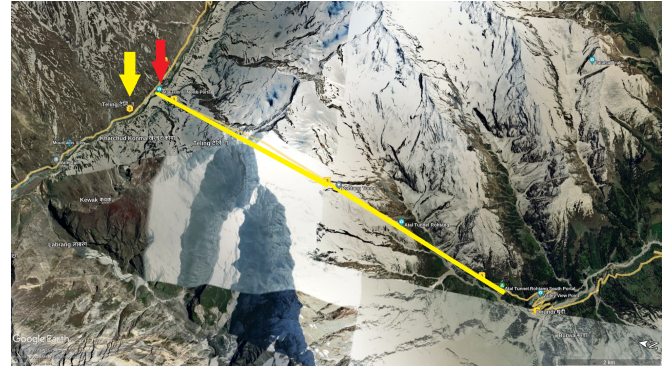


Figure 1: Teling Nala and Teling village (yellow arrow on the left) near the North portal of Atal tunnel (red arrow to the right). *Courtesy: Google Earth satellite imagery.*

avalanches are a frequent natural occurrence in the Indian Himalayas encompassing two union territories and three states that are avalanche prone. These regions include the union territories of Jammu and Kashmir, Ladakh, and the states of Himachal Pradesh, Uttarakhand, and Sikkim, where avalanche incidents are prevalent.

Not much work has been carried out on modeling and simulation of avalanche dynamics in the Indian Himalayas owing to the sheer scale of the region and the expensive nature of such computational simulations. Only a few studies on specific sites have been performed [7]. The use of computational fluid dynamics (CFD) has not been explored much for the risk analysis of avalanche sites in the Indian context.

The present study focuses on the computational modelling of snow avalanche dynamics of the Teling Nala site located near the North portal of the Atal tunnel, which was constructed in 2020 on the Manali–Leh highway in Himachal Pradesh. The tunnel was constructed to reduce travel time between Manali and Keylong leading to significant growth in tourism during both the winter and summer seasons. Teling Nala, as shown in Figure 1, encounters frequent avalanches in the winter and spring months risking life at the Teling village and causing road closures.

This work presents a case study of computational modeling of snow avalanche dynamics of the Teling Nala site. Given the large extent of the domain (ranging in kilometers), a computationally-tractable approach was adopted. Mass and momentum equations were integrated along the vertical

direction resulting in the so-called depth-averaged equations [4], which were closed using the Mohr-Coulomb rheology [6]. Additionally, adaptive mesh refinement was used to dynamically resolve details near the flowing heap, ensuring the best utilization of computational resources.

This case study presents and analyses a few scenarios which include a range of parameters such as the internal friction angle (ϕ) and the bed friction angle (δ), a range of volumes of the initial pile, and two potential starting zones (located at ~ 5500 m a.s.l.), as shown in Figure 2.

In section II, equations used in the depth-averaged approach are discussed, followed by the numerical techniques used. The section also presents benchmarking of the model against published work for Makunosawa valley in Japan [8]. In section III, results of numerical modeling of snow avalanche dynamics at the Teling Nala site are presented. Parametric study and sensitivity analysis are discussed. Mean velocity of the heap and runout distance of the avalanche are analyzed for all cases. Finally, a worst-case scenario is discussed where an avalanche initiates simultaneously from two locations, as highlighted in Figure 2. Key conclusions and scope for future work are presented in Section IV, highlighting the importance of the choice of correct bed friction angle.

II. METHODOLOGY

A. Depth-averaged equations

For shallow flows, the depth-averaged method has proven to be a favourable approximation. In this method, the flow variables are integrated along a direction normal to the local topography, resulting in a reduced number of dimensions, making the set of model equations tractable. The depth-averaged continuity equation is given as:

$$\frac{\partial h}{\partial t} + \frac{\partial}{\partial x}(hu) + \frac{\partial}{\partial y}(hv) = 0. \quad (1)$$

Here, $h(x, y, t)$ is the snow depth along the normal direction z in the curvilinear (local) orthogonal coordinate system. The local coordinate x is along the downslope direction and y is perpendicular to x in the flow plane. Here, u and v are the depth-averaged velocity components in the x and y directions, respectively. It must be noted that the flow is considered incompressible.

The depth-averaged momentum equations in x and y directions are obtained as:

$$\frac{\partial}{\partial t}(hu) + \frac{\partial}{\partial x}(hu^2) + \frac{\partial}{\partial y}(huv) = hgs_x - \frac{\partial}{\partial x}\left(\frac{\beta_x h^2}{2}\right) \quad (2)$$

$$\frac{\partial}{\partial t}(hv) + \frac{\partial}{\partial x}(huv) + \frac{\partial}{\partial y}(hv^2) = hgs_y - \frac{\partial}{\partial y}\left(\frac{\beta_y h^2}{2}\right) \quad (3)$$

Here, s_x and s_y are the accelerations that propel the flow in the corresponding directions, which are given as:

$$s_x = \sin \zeta - \frac{u}{|\mathbf{u}|} \tan \delta \left(\cos \zeta + \lambda \kappa \frac{u^2}{g} \right) - \epsilon \cos \zeta \frac{\partial b}{\partial x}, \quad (4)$$

and

$$s_y = -\frac{v}{|\mathbf{u}|} \tan \delta \left(\cos \zeta + \lambda \kappa \frac{u^2}{g} \right) - \epsilon \cos \zeta \frac{\partial b}{\partial y}. \quad (5)$$

The Mohr-Coulomb rheology is used to model the tangential stress in this work, which is shown to work well for cohesionless (dry) avalanches. In addition, the model assumes a hydrostatic pressure distribution. The non-dimensional number ϵ represents a ratio of the height of flow to its width in the flow plane, and λ is the ration of flow width to the radius of curvature of the topography. Angle ζ is the angle the normal makes with z -direction and δ is the bed friction angle. In the above expressions, b represents the bottom profile.

In Eqs. (2) and (3), β_x and β_y are given as:

$$\beta_x = \epsilon \cos \zeta K_x \quad (6)$$

and

$$\beta_y = \epsilon \cos \zeta K_y, \quad (7)$$

with the earth pressure coefficients:

$$K_x = 2 \sec^2 \phi \{1 \pm (1 - \cos^2 \phi \sec^2 \delta)^{0.5}\} - 1, \quad (8)$$

and

$$K_y = \frac{1}{2} \left\{ K_x + 1 \mp ((K_x - 1)^2 + 4 \tan^2 \delta)^{0.5} \right\}. \quad (9)$$

The upper sign is activated in case of active state and the lower sign in case of passive state. Angle ϕ denotes the internal friction angle. Further details of the equations can be found in Pudasaini and Hutter [4].

Initial pile details were specified through initial condition for the pile height h . Zero mass flux boundary conditions were used on all boundaries.

B. Solution method

The finite-volume method with a first-/second-order Godunov's scheme was used to solve the governing equations (Eqs. (1)–(3)). The TITAN2D open-source code [3], which makes use of adaptive mesh refinement (AMR) was used.

AMR dynamically adjusts the mesh resolution in regions where heap is flowing, resulting in increased accuracy at low computational cost when compared with fixed meshes. The combination of the depth-averaged approach with AMR offers a tractable solution method for numerically modeling snow avalanches on actual mountain slopes.

C. Benchmarking

The computational method used in this work was first benchmarked for the simulation of a snow avalanche on a real mountain slope, against published work available in literature. The terrain model was developed from the data obtained from the Advanced Spaceborne Thermal Emission and Reflection Radiometer (ASTER) Global Digital Elevation Model (DEM), which has a spatial resolution of 30 m. The simulation setup details, including the details of the initial pile and rheological parameters, are given in Table 1. The initial pile projection was approximated as an ellipse with major and minor axes as shown in Table 1, with static snow of height 2 m.

In the initial stages, the avalanche accelerated because of the steep slope in the Makunosawa valley. Consequently, it started to decelerate as the slope decreased and came to rest after covering a distance of ~ 3000 m. It must



Figure 2: The Teling Nala gully shown in yellow vertical line down the slope. The two arrows show two potential starting zones of the avalanche. Teling gully meets the road downstream of the Teling village. Courtesy: Google Earth satellite imagery.

Table 1: Model parameters used in benchmarking

Parameter	Value
Internal friction angle (ϕ)	20°
Bed friction angle (δ)	13°
Snow depth of the initial pile (h)	2 m
Major axis of the initial pile	250 m
Minor axis of the initial pile	100 m

be noted that ‘distance’ in this work refers to projected distance, not actual distance travelled on the 3-D terrain. Figure 3 shows a plot of the volume-average pile velocity with the average (projected) distance traveled by the pile centroid. A satisfactory agreement with the simulations of Takeuchi et al. (2018) [8] can be seen with a similar trend in both plots. The runout distance, which is the distance at which the avalanche stops, was off by 150 m for the present simulations, which is 5% of the overall distance traveled by the heap. The maximum value of the volume-average velocity was underpredicted by 10% in the present work. The above differences can be attributed to the approximation of the position of the center of the initial heap, which was not specified exactly in the benchmark paper. Takeuchi et al. (2018) [8] found a good agreement of their numerical results with field avalanche data for a bed friction angle of 13°-14° for the avalanche path and runout distance. Acceptable

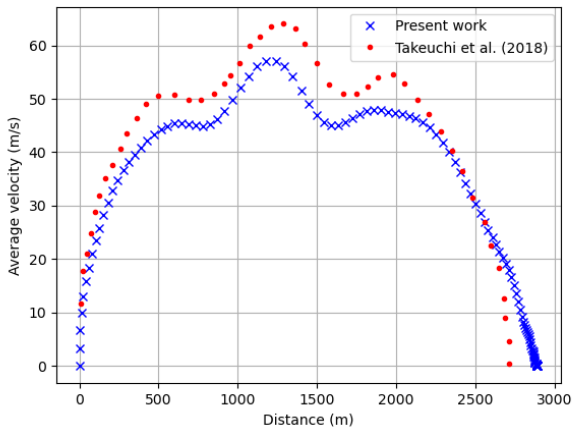


Figure 3: Benchmarking of the results of snow avalanche dynamics at Makunosawa Valley, Japan against the work of Takeuchi et al. [8].

benchmark results were the motivation to apply the present method for analyzing snow avalanche dynamics in the Indian Himalayas, as discussed in the next section.

III. RESULTS AND DISCUSSION

Results of the numerical analysis of snow avalanche dynamics at Teling Nala are presented in this section. Meshed domain is shown in Figure 4 at three time instances. The mesh adapting to the pile height field can be clearly seen from the figure. The variations of parameters such as internal friction angle (ϕ) and bed friction angle (δ), and the volume of initial pile are considered on the velocity and runout distance of the avalanche.

For the present study, two values— 30° and 40° —of internal friction angle were used based on chute studies in nearby regions of Teling Nala [1]. Three bed friction values were chosen— 15° , 20° and 25° [5]. The snow depth near the South portal of the Atal Tunnel has been reported to range between 0.84 m and 1.24 m [2], therefore, an initial pile height of 0.9 m, 1 m, and 1.2 m were chosen in the current work. The above choices resulted in a collection of scenarios which were run on a machine with Intel i7-9700K processor, which clocks at 3.6 GHz, along with a total memory of 48GB. Each simulation took less than 5 minutes to complete on this machine.

Figure 5 presents the effect of internal friction angle on avalanche dynamics, keeping the bed friction angle and initial pile height the same. The volume-average velocity and runout distance of the avalanche are nearly the same, suggesting limited dependence on the internal friction angle, similar to the findings of Pudasaini and Hutter [4].

In the next analysis, the impact of altering the bed friction angle was examined on avalanche flow parameters. Both, the volume-average velocity of the pile and the runout distance were significantly affected with bed friction angle, as visible in Figure 6. In fact, the output estimates are highly sensitive to the bed friction angle, as shown in Figure 7, which shows the sensitivity analysis of bed friction angle on velocity and runout estimates. One degree change in the bed friction angle resulted in around 75% change in maximum velocity estimate and 25% change in runout distance. The bed friction angle represents the resistance to shear within the interaction between the snow and the underlying terrain. If the surface is rough (indicate high bed friction angle), the avalanche will experience more resistance as it flows. A visual representation of the impact of the three cases presented in Figure 6 is shown in Figure 8 where the avalanche track is shown to follow the Teling stream gully. It can be noticed that an increase in the bed friction angle above 20° prevented the heap from reaching Teling village.

Thirdly, the effect of initial pile volume was studied. The initial volume was controlled by modifying the pile height keeping its elliptical footprint the same. Figure 9 shows the impact of the volume of initial pile on the volume-average velocity and runout distance of the avalanche. For the volumes in ratio 0.9 : 1.0 : 1.2, there is no significant impact on the dynamics of avalanche. However, a small increase in the velocity and runout is noticed for the largest volume, as expected. In addition, Figure 10 presents the maximum height of the heap at various times corresponding to the (projected) distance of the centroid of the heap. The largest initial volume showed the maximum height as

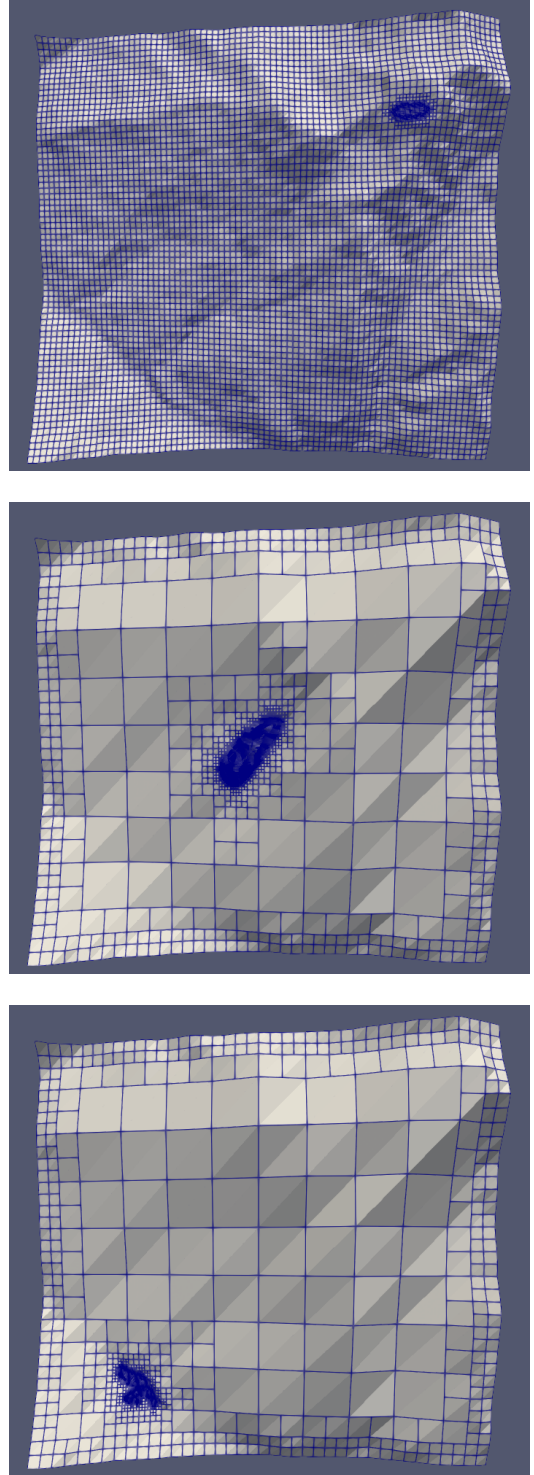


Figure 4: Meshed domain for the Teling Nala avalanche at (a) $t = 0$ s, (b) $t = 60$ s, and (c) $t = 180$ s. Adaptive meshes can be clearly seen.

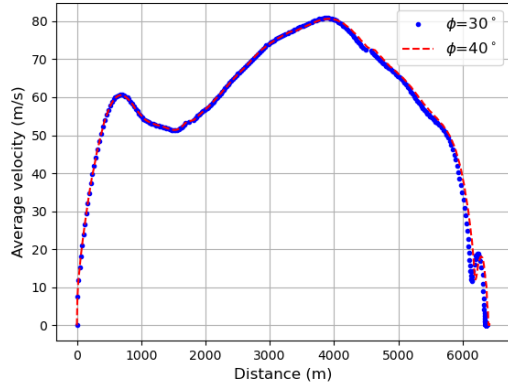


Figure 5: Effect of the internal friction angle (ϕ). Volume-average velocity is plotted against the projected distance traveled by the avalanching mass. Bed friction angle was 15° and the initial snow depth was chosen as 0.9 m.

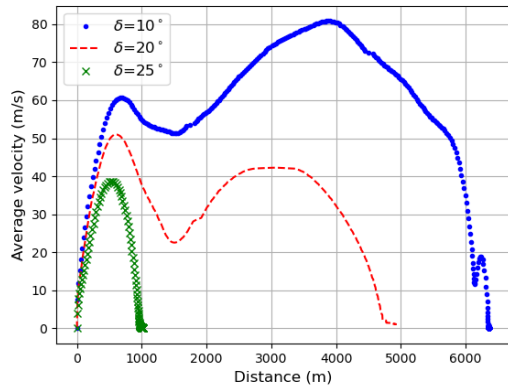


Figure 6: Effect of the bed friction angle (δ) on volume-average avalanche velocity and runout distance. All cases were simulated for $\phi = 30^\circ$ and initial snow depth = 0.9 m.

expected. Towards the end, as expected, the runout pile heaps up resulting in an increase in height, however, after piling up, the heap started spreading laterally on the road resulting in a lower height towards the end. The arrow in the figure denotes the Teling village where the height and average velocities have significant magnitudes indicating the dangerous nature of the avalanche for the village residents.

Finally, a worst-case scenario was conceived wherein the avalanche was triggered simultaneously at the two starting zones, as shown in Figure 2. The total volume in this case was 2.6 times the volume for a single initiation zone with the same initial snow depth of 1.2 m. The internal friction angle and bed friction angle values were taken as 30° and 15° , respectively. From Figures 11 and 12 it can be seen clearly that the avalanche almost came to rest when it reached the Teling village.

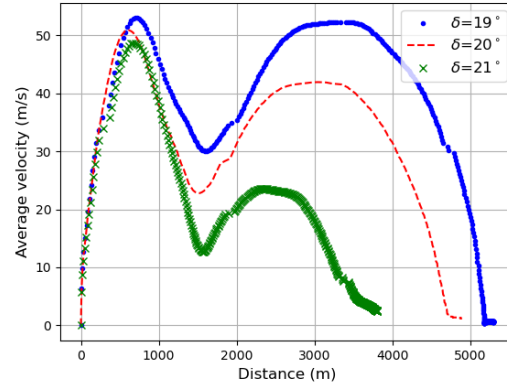


Figure 7: Sensitivity analysis for the bed friction angle (δ).

IV. CONCLUSIONS

In this paper computational modelling of snow avalanche dynamics was presented. The depth-averaged model with the Mohr-Coulomb rheology was first benchmarked for avalanche flow in Makunosawa valley, Japan using the open-source TITAN2D code. The overall trend of volume-average mean velocity with respect to the distance travelled was predicted well.

The model was then applied for the numerical study of snow avalanche in the Teling Nala site, which is critically placed near the North portal of the Atal tunnel in the Indian Himalayas. Parametric study for internal and bed friction angles, along with an effect of the initial volume of avalanching pile were carried out. It was observed and concluded that that bed friction angle has significant effect on the mean velocity as well as the runout distance of the snow avalanche. Good estimates of bed friction angle can be useful in identifying high risk regions through the use of such depth-averaged model simulations. The results were not sensitive to the (range of chosen) internal friction angles. Although the range of the volume chosen for the initial pile showed minimal effect on the flow dynamics, however, large volume avalanches can be dangerous due to the energy and momentum they carry and can cause significant loss to life and property. Numerical simulations help identify the path of an avalanche, aiding in the identification of areas prone to avalanche damage.

In addition, 3-D time snapshot visualisations for a worst-case scenario were also presented. This research contributes to the present understanding of avalanche behaviour at the Teling Nala site which can be utilised for designing avalanche defense structures and conducting a hazard analysis of the region. It is concluded that computational approach using depth-averaged modelling and adaptive mesh refinement provides a tractable method for analysing avalanche dynamics at key sites such as the one chosen in this work.

ACKNOWLEDGEMENTS

VS expresses his gratitude to the Ministry of Education

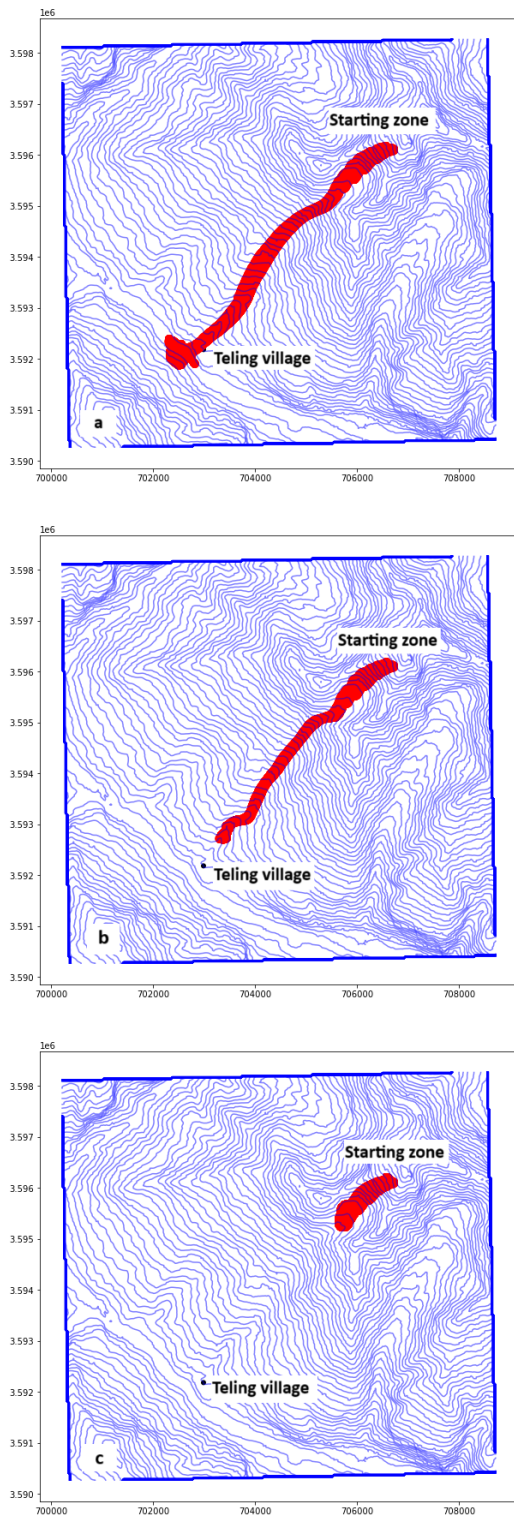


Figure 8: Visual representation of avalanche track on contour of the Teling gully region. Avalanche height > 0.1 m is highlighted in red at 800 iteration intervals. The axes markings are UTM coordinates. Results for bed friction angles of (a) 15° , (b) 20° , and (c) 25° are shown.

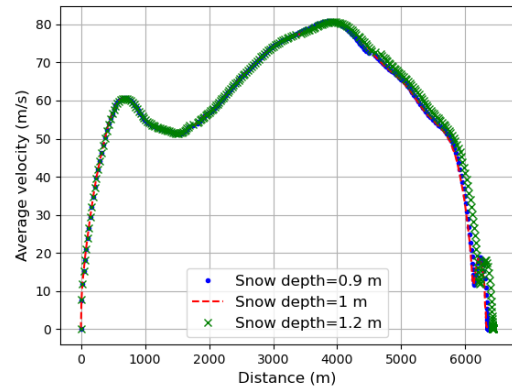


Figure 9: Effect of initial volume of pile on average snow velocity; $\phi = 30^\circ$ and $\delta = 15^\circ$.

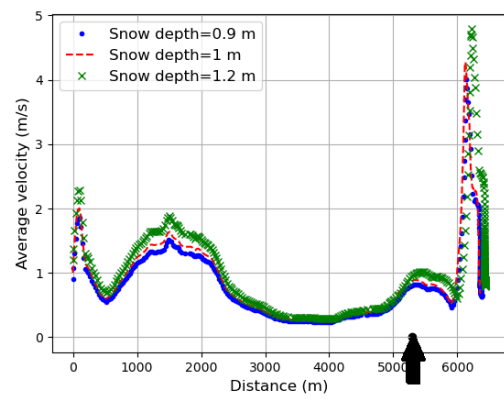


Figure 10: Effect of initial volume of pile on maximum pile height; $\phi = 30^\circ$ and $\delta = 15^\circ$. Arrow represents the position of Teling village.

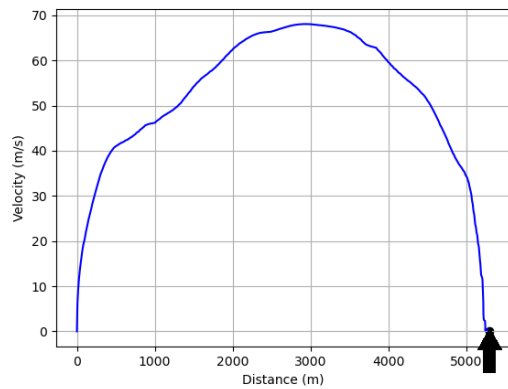


Figure 11: Worst-case scenario: mean velocity with distance. Arrow indicates the location of Teling village.

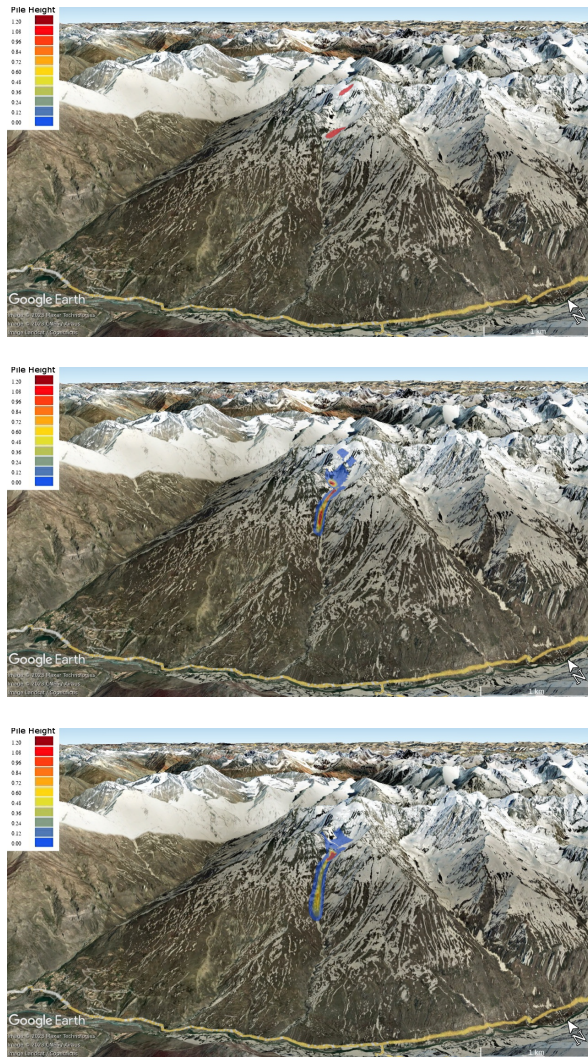


Figure 12: Time snapshots of avalanche path for the worst-case scenario.

(MoE), India for providing him with the scholarship for his PhD studies. VS also would like to thank his colleague Yuvraj Aseri who provided support through valuable discussions in the initial stage of this work.

REFERENCES

[1] RK Aggarwal and A Kumar, *Application of CFD code for simulation of an inclined snow chute flow*, Int. J. Eng. Res. Appl **3** (2013), no. 2, 10.

[2] S Awasthi, S Kumar, PK Thakur, K Jain, A Kumar, and Snehmami, *Snow depth retrieval in north-western Himalayan region using pursuit-monostatic TanDEM-X datasets applying polarimetric synthetic aperture radar interferometry based inversion modelling*, Int. J. Remote Sens. **42** (2021), no. 8, 2872–2897.

[3] A Patra, AC Bauer, CC Nichita, EB Pitman, MF Sheridan, M Bursik, B Rupp, A Webber, AJ Stinton, LM Namikawa, et al., *Parallel adaptive numerical simulation of dry avalanches over natural terrain*, J. Volcanol. Geotherm. Res. **139** (2005), no. 1-2, 1–21.

[4] SP Pudasaini and K Hutter, *Avalanche dynamics: dynamics of rapid flows of dense granular avalanches*, Springer Science & Business Media, 2007.

[5] A Sattar, S Allen, M Mergili, W Haeberli, H Frey, AV Kulkarni, UK Haritashya, C Huggel, A Goswami, and R Ramsankaran, *Modeling potential glacial lake outburst flood process chains and effects from artificial lake-level lowering at gepang gath lake, indian himalaya*, J. Geophys. Res. F: Earth Surf. **128** (2023), no. 3.

[6] SB Savage and K Hutter, *The motion of a finite mass of granular material down a rough incline*, J. Fluid Mech. **199** (1989), 177–215.

[7] DK Singh, VD Mishra, and HS Gusain, *Simulation and analysis of a snow avalanche accident in lower western himalaya, india*, J. Indian Soc. Remote Sens. **48** (2020), no. 11, 1555–1565.

[8] Y Takeuchi, K Nishimura, and A Patra, *Observations and numerical simulations of the braking effect of forests on large-scale avalanches*, Ann. Glaciol. **59** (2018), no. 77, 50–58.